

Parallel Cluster Labeling for Large-Scale Monte Carlo Simulations

M. Flanigan* and P. Tamayo
Thinking Machines Corp.
Cambridge, MA 02142.

August 15, 2018

ABSTRACT

We present an optimized version of a cluster labeling algorithm previously introduced by the authors. This algorithm is well suited for large-scale Monte Carlo simulations of spin models using cluster dynamics on parallel computers with large numbers of processors. The algorithm divides physical space into rectangular cells which are assigned to processors and combines a serial local labeling procedure with a *relaxation* process across nearest-neighbor processors. By controlling overhead and reducing inter-processor communication this method attains good computational speed-up and efficiency. Large systems of up to 65536^2 spins have been simulated at updating speeds of 11 nanosecs/site (90.7×10^6 spin updates/sec) using state-of-the-art supercomputers. In the second part of the article we use the cluster algorithm to study the relaxation of magnetization and energy on large Ising models using Swendsen-Wang dynamics. We found evidence that exponential and power law factors are present in the relaxation process as has been proposed by Hackl *et al.* The variation of the power-law exponent λ_M taken at face value indicates that the value of z_M falls in the interval $0.31 - 0.49$ for the time interval analysed and appears to vanish asymptotically.

* Current Address: GSIA, Carnegie-Mellon University, Pittsburgh, PA 15213.

1. Introduction.

Over the last twenty years Monte Carlo simulations have become an important and reliable calculation method in Statistical Mechanics and Field Theory [1-4]. Large-scale high-resolution Monte Carlo simulations have provided means to compute critical exponents, transition temperatures, cumulants and other critical properties with unprecedented accuracy[5-20].

Efficient cluster labeling algorithms are needed for large-scale simulations of spin models using cluster dynamics[21, 22] and other physical systems such as percolation clusters, nucleation droplets, polymers, fractal structures, and particle tracks. Cluster labeling is related to the problem of finding the connected components of a graph, which has applications in computer vision, image processing and network analysis, among others.

Many general parallel algorithms for finding connected components have been introduced in the Computer Science literature [23-37]. Most of these methods are designed for SIMD architectures using high-level language algorithmic descriptions. These algorithms can be used for lattice problems, such as in the case of image processing, but are not well suited for large-scale Monte Carlo simulations which require the repeated labeling of complicated structures (fractals). The main problem with these general methods is their absolute performance when implemented in real parallel computers.

Over the last five years a number of SPMD (Single Program Multiple Data) parallel cluster labeling methods for Monte Carlo simulations have been introduced [8, 10, 15-20]. These methods have attained scalability with different degrees of success. A few of these methods are scalable and can be used with large numbers of processors[10, 16, 18, 19]. SIMD and vector cluster labeling algorithms explicitly designed for Monte Carlo simulations have also been introduced [10-13, 38] but their absolute performance still lags behind the one attained by the best SPMD algorithms.

In this paper we present an optimized version of a SPMD relaxation-based algorithm introduced in ref. [16]. The algorithm is general and can be applied to higher dimensional systems. We will concentrate on the problem of cluster labeling for the 2D Ising Model with Swendsen-Wang dynamics[21]. A percolation process[14] is used to define bonds between aligned spins. The bonds are thrown with probability $p_{bond} = 1 - e^{-2\beta}$, and the clusters of connected spins, the Coniglio-Klein[39, 40] percolation clusters, are flipped with 50% probability. At the critical point the clusters span the system and labeling information has to propagate across the entire computational domain. The basic algorithm is discussed in ref. [16] and here we will give a brief review of the improved version and present new data. In the second part of the paper we will show new results of the application of the algorithm to study the relaxation of large 2D Ising models.

2. Description of the Algorithm.

Physical space is divided into rectangular cells in such way that each cell is assigned to one processor (see Fig. 1). The algorithm labels the clusters in two stages: first it finds all the clusters inside each processor using a serial algorithm, and then it performs a global relaxation process where processors exchange clusters labels with nearest neighbors until a fixed point is reached. The operations of the algorithm are shown in Figs. 2 and 3. The Cluster-Labeling procedure can be described as follows:

Procedure Spin-Dynamics & Cluster-Labeling:

- (i) Define connectivity for the sites (spins) by throwing the Swendsen-Wang percolation bonds.

- (ii) Apply a serial algorithm (see procedure Local-Labeling below) to label the clusters inside each processor independently. At boundary sites the off-node bonds are ignored for now. At the end all sites are labeled with their “local root” labels which are then globalized (i.e. made unique over the whole system).
- (iii) Iterate several relaxation cycles (see procedure Relaxation below), exchanging local root labels with neighboring processors until all processors detect no change in the labels. At the end all sites get their final global label from their local roots.
- (iv) Clusters of spins are flipped with 50% probability and measurements of relevant quantities are accumulated (energy, magnetization etc.).

The serial local algorithm we used in ref. [16], and which is based on the Hoshen-Kopelman[41] algorithm, was somewhat inefficient in terms of cache memory utilization and other implementation-dependent characteristics. To improve it we explored different variations of it until we found one that is significantly better. This particular serial algorithm can be described as follows.

Procedure Local-Labeling: (cluster labels are used as “pointers” to local sites.)

- (i) All sites are initialized with a unique label (i.e. each site points to itself).
- (ii) For each site do the following, starting from the north-west corner and moving down row-wise:
 - (a) If the neighbor to the north is connected then follow the label pointer until the root is found (site pointing to itself). If the root label is less than the current label then set the current label (and current root) to the root label.
 - (a) If the neighbor to the east is connected set its label to the current label.
- (iii) After this has been done for all nodes then do a final collapse of the connectivity trees, defined by the previous operations, by making every site point to the root label of the cluster it belongs to.

The connections across processor boundaries are ignored during the local labeling. Once the local labeling has been completed (see Fig. 2) a number of relaxation cycles are iterated in order to label the clusters globally (across processors). Each cycle consists of interchanging, comparing and resetting labels with neighboring processors. The relaxation procedure consists of the following:

Procedure Relaxation:

- (i) A preparation step is executed to set up a list of pointers to the local roots on each node boundary (see last panel in Fig. 2).
- (ii) A number of relaxation steps are iterated. To do this each processor interchanges boundary labels with the neighbors in each direction for those boundary sites which have connections off processor. The labels are sent in a single block of data using standard message-passing calls. The local root labels are compared with the ones received from the neighbors and then set to the minimum values. This is done for the four directions (north, east, south, west) before checking for the termination condition (all nodes detect no change in the labels).

We found that this algorithm is well suited for Monte Carlo simulations and that even for large numbers of processors the time spent on the relaxation cycles is relatively small. The relaxation procedure appears to be a wasteful operation at first sight; however, the algorithm is efficient because communications are done by exchanging large blocks and the label comparison and resetting overhead is kept to a minimum. The connectivity of the “renormalized” processor-grid lattice is much simpler than that of the original system and therefore the relaxation process converges very quickly. Total execution times are dominated by local labeling not by communications. All these results in good scaling and performance. As we will see in the next section this algorithm can attain updating speeds of about 90 million spin-updates per second, on a 256-node CM-5E, and is considerably faster than comparable algorithms on vector supercomputers[42, 13]. Surprisingly enough it is even faster than some of the high-performance single-spin flip algorithms using multi-spin coding[43].

2. Scaling and Numerical Results.

Taking into account the fact that the cluster labeling algorithm operates at the core of equilibrium Monte Carlo simulations one has to worry more about average than worst case performance. The probability of obtaining a given configuration of clusters is determined by the Boltzmann weight of that configuration. The probability of observing the worst case is negligible. On the other hand, “typical” configurations often contain fractal structures which are relatively hard to label.

In order to make a meaningful scaling analysis one has to concentrate on average execution times defined over critical equilibrium Monte Carlo configurations. A detailed complexity and scaling analysis was presented in ref. [16]. Here we will review the main results.

The total time to perform the cluster labeling consists of two contributions: a “local time”, the time spent by the serial algorithm inside each processor, and a “relax time” which is the time spent in the global relaxation procedure until completion,

$$T_{parallel} = T_{local} + T_{relax} = an + bp^{d_{min}/2}n^{1/2}, \quad (1)$$

where $n = l \times l$ is the size for the subsystem assigned to each processor, a and b are constants that characterize the computation and communication rates for a given machine, and p is the total number of processors. The scaling of the local part is assumed to be basically $O(n)$. In principle it is $O(n \log^* n)$ but, as is discussed it ref. [24], $\log^* n$ can be safely considered a constant. The exponent d_{min} is the *chemical distance* exponent that plays the role of a dynamical critical exponent for the labeling process[44, 45, 16]. If n is large compared with p , and the communication to computation ratio a/b is small, the scaling will be dominated by the local part. This can be better seen by analyzing the speed-up function $S(n, p)$, which is the ratio between the serial and parallel times,

$$S(n, p) = \frac{T_{serial}}{T_{parallel}} = \frac{anp}{an + bp^{d_{min}/2}n^{1/2}}. \quad (2)$$

The speed-up improves with large n and gets worse as p increases. The speed-up as a function of p for fixed total system size N is given by,

$$S_N(p) = \frac{aNp}{aN + bp^{(d_{min}+1)/2}N^{1/2}}, \quad (3)$$

and the corresponding efficiency $E_N(p) = S_N(p)/p$ is,

$$E_N(p) = \frac{1}{1 + \frac{b}{a}[p^{(d_{min}+1)}N^{-1}]^{1/2}}. \quad (4)$$

The efficiency decreases as the number of processors increases because inter-processor communication times eventually dominate. In practice, it is important to make b/a as small as possible to reduce absolute times. The efficiency is a universal function of $p^{(d_{min}+1)}N^{-1}$ and therefore the only important parameter in the simulation, from a computational point of view, is the value of $p^{(d_{min}+1)}N^{-1}$. The larger N is in relation to p , the better the algorithm will perform.

Our implementation of the algorithm was done using standard C language plus message-passing calls (CMMD library) on the CM-5E supercomputer. We measured execution times for different total system sizes N and numbers of processors p for 2D Ising Swendsen-Wang simulations. We obtained: $a = 2.79 \times 10^{-6}$ secs. and $b = 6.2 \times 10^{-6}$ secs., and therefore $b/a = 2.22$. The timings are shown in Table I.

Fig. 4 shows local, relax, and total times for different system sizes on a 64-node CM-5E. Measurements times (energy, magnetization, etc.) were not included. As we can see in the figure, local times dominate except for small N . Typical updating times are of the order of 40 nanosecs/site and 10 nanosecs/site for 64 and 256 node CM-5E machines respectively.

Table I: Timings for 2D Swendsen-Wang dynamics on CM-5E supercomputers.

System Size N	number of procs. p	Local time [secs]	Relax time [secs]	Total time [secs]	Speed [10^6 spin updates/sec]	Time/site [nanosecs]
128 ²	32	0.0012	0.0014	0.0026	6.3	164
256 ²	32	0.005	0.002	0.007	9.4	104
512 ²	32	0.020	0.003	0.023	11.3	88.3
1024 ²	32	0.078	0.007	0.085	12.3	81.1
2048 ²	32	0.312	0.017	0.329	12.7	78.5
4096 ²	32	1.24	0.04	1.28	13.1	76.5
8192 ²	32	5.15	0.08	5.23	12.8	78.0
16384 ²	32	22.19	0.16	22.4	12.0	83.3
256 ²	64	0.002	0.002	0.004	15.2	66.4
512 ²	64	0.010	0.003	0.013	20.2	48.2
1024 ²	64	0.039	0.006	0.045	23.3	42.5
2048 ²	64	0.157	0.013	0.169	24.8	40.4
4096 ²	64	0.623	0.027	0.650	25.8	38.7
8192 ²	64	2.580	0.060	2.640	25.4	39.3
16384 ²	64	11.12	0.12	11.24	23.9	41.9
32768 ²	64	46.27	0.24	46.52	23.1	43.3
512 ²	256	0.002	0.004	0.006	41.6	24.02
1024 ²	256	0.009	0.006	0.015	69.4	14.41
2048 ²	256	0.037	0.011	0.048	87.2	11.47
4096 ²	256	0.149	0.021	0.170	98.5	10.15
8192 ²	256	0.596	0.049	0.645	104	9.61
16384 ²	256	2.430	0.096	2.520	106	9.40
32768 ²	256	10.63	0.105	10.73	100	9.99
65536 ²	256	47.10	0.261	47.36	90.7	11.0

For very large systems the performance decreases slightly due to decreased cache memory usage. This effect is not taken into account in the scaling model. Simulating a 32768² (65536²) system requires about 84 Mbytes of local memory on a 64 (256) node CM-5E. This is about 5 bytes per site: 4 bytes (one integer) for the label and one byte for the spin. The scaling behavior of the model agrees well with the actual measured times. The local

times scale linearly with n , and the relaxation times with $n^{1/2}$ as expected. The speed-up $S_N(p)$, as a function of the number of processors for different system sizes, is shown in Fig. 5. Notice that even for small system sizes, such as $L = 512$, the speed-up increases without saturation even for p equal to 256 processing nodes. The 32768^2 and 65536^2 lattices are simulated with more than 99% efficiency on 64 and 256 processors respectively. The efficiency $E_N(p) = S_N(p)/p$ as a function of p is shown in Fig. 5. When these points are plotted as a function of $[p^{(d_{min}+1)}N^{-1}]^{1/2}$, as shown in Fig. 6, they show the universal scaling behavior predicted by Eq. 4: data for different system sizes and number of processors collapses reasonably well to a single curve.

The relaxation method can be extended in a hierarchical style, for example using the multi-grid approach introduced in ref. [11], but in practice this is unnecessary because nearest neighbor relaxation is a very efficient operation for global labeling even on large processor grids.

3. Relaxation of Large 2D Ising Model with Swendsen-Wang Dynamics.

In this section we present results of a study of the relaxation of magnetization and energy on large 2D Swendsen-Wang Ising models. The typical simulation consists of setting all spins up and then letting the system relax to equilibrium at T_c . Several relaxation experiments are performed to obtain significant statistics. When enough data is available different scaling models can be tested and the value of z estimated. This method has been used for local Ising dynamics in two and three dimensions by Stauffer[14], Stauffer and Kertesz[46] and Miranda[45]. Stauffer and Kertesz[15] simulated large Swendsen-Wang Ising systems with up to 6400^2 spins and found large corrections to scaling and finite size effects. They also found that the time dependent exponent $z(t)$ vanishes linearly in $1/t$ implying $z = 0$ in agreement with previous results of Heermann and Burkitt[8], and others. Tamayo[9] performed a similar analysis with systems up to 32768^2 spins and found relaxation behavior for intermediate and large times which was consistent with a power law decay and $z = 0.25 \pm 0.05$. Later, Hackl *et al* [19] studied systems with up to 17920^2 spins and proposed a relaxation ansatz combining power law and exponential behavior. They found that this ansatz was able to fit the data reasonably well and explained the difference in the behaviors observed by Stauffer and Kertesz[15] and Tamayo[9]. Their power law exponents correspond to $z_M = 0.43$ and $z_E = 0.44$. These values are higher than the value $z_M = 0.25$ found by Tamayo, however a comparison of Hackl *et al*'s raw relaxation data with Tamayo's showed good agreement[47].

In order to better understand the nature of these differences and explore the complex relaxation of energy and magnetization we performed relaxation experiments with large $2D$ systems with $L = 2048$, $L = 16384$ and $L = 32768$ spins. Each experiment consisted of setting all spins up and letting the system run for 100 Swendsen-Wang time steps with the temperature set to T_c . In total we performed 5,000 relaxation experiments for $L = 2048$, 210 for $L = 16384$ and 46 for $L = 32768$. Our analysis will focus on the data for the $L = 32768$ system.

Figs. 8 and 9 show the average magnetization and energy as a function of time for different lattices. For short times the relaxation is basically the same for all lattice sizes but for longer times is different due to finite size effects. The behavior at short times appears to be dominated by an exponential factor as was observed by Kertesz and Stauffer[15]. At intermediate and longer times the behavior appears to be dominated by a power law[9]. To account for this exponential/power-law phenomenology Hackl *et al* proposed an ansatz combining exponential and power law decay[19],

$$M(t) \sim (t + \Delta_M)^{-\lambda_M} e^{-b_M t} \quad (5)$$

and similarly for the energy,

$$E(t) \sim (t + \Delta_E)^{-\lambda_E} e^{-b_E t}. \quad (6)$$

If one considers an overall amplitude in addition to b_M , λ_M and Δ_M the model has 4 parameters. In order to fit this model to Monte Carlo data Hackl *et al* found useful to define the following auxiliary functions,

$$h_M(t) = -\frac{1}{M(t)} \frac{dM(t)}{dt} \quad (7)$$

and

$$g_M(t) = -\frac{1}{h_M(t+2) - h_M(2)}. \quad (8)$$

These functions can be expressed in terms of Δ_M , b_M and λ_M as follows,

$$h_M(t) = \frac{\lambda_M}{t + \Delta_M} + b_M \quad (9)$$

$$g_M(t) = \frac{1}{\lambda_M} \left[\frac{(\Delta_M + 2)^2}{t} + \Delta_M + 2 \right]. \quad (10)$$

Analogous equations can be defined for the energy. The reason for this reformulation is that g_M ($g_E(t)$) is independent of b_M (b_E) and then a standard linear fit can be done for g_M (g_E) vs $1/t$. In this linear fit the slope and intercept correspond to $1/\lambda_M(\Delta_M + 2)^2$ and $1/\lambda_M(2 + \Delta_M)$ respectively. Hackl *et al* fitted this model to their data and found the following values for the parameters[19]: $b_M = 0.0043 \pm 0.0010$, $\lambda_M = 0.29 \pm 0.03$, and $\Delta_M = 4.5 \pm 0.6$ for the magnetization and $b_E = 0.0281 \pm 0.0020$, $\lambda_E = 2.26 \pm 0.08$, and $\Delta_E = 5.9 \pm 0.25$ for the energy.

The exponent b_M (b_E) was obtained using the values of λ_M (λ_E) and Δ_M (Δ_E) to calculate the function,

$$\tilde{b}_M(t) = \lambda_M \log \left[\frac{t + 1 + \Delta_M}{t + \Delta_M} \right] + \log \left[\frac{M(t+1)}{M(t)} \right], \quad (11)$$

and averaging $\tilde{b}_M(t)$ ($\tilde{b}_E(t)$) over long times where it is roughly constant. Another way in which they obtained b_M (b_E) is by imposing the condition $M(t=0) = 0$ and $E(t=0) = -2$ on the ansatz,

$$b_M(t) = -\frac{1}{t} \left[\log \frac{M(t)}{M(0)} + \lambda_M \log \frac{t + \Delta_M}{\Delta_M} \right], \quad (12)$$

and then averaging the roughly constant $b_M(t)$ ($b_E(t)$) for intermediate and long times.

The exponential/power-law ansatz fitted their data reasonably well. From the values of λ_M and λ_E they also computed values for z using the following relations,

$$\lambda_M = \beta/\nu z \quad (13)$$

$$\lambda_E = (1 - \alpha)/z, \quad (14)$$

which produced $z_M = 0.43$ and $z_E = 0.44$. They did not find evidence of a logarithmic factor in the energy.

In our study we followed a similar methodology. We analyzed data from 46 relaxation experiments with the 32768^2 system. Figs. 8 and 9 show the raw relaxation data for energy and magnetization on three different lattice sizes. From these plots we obtained instantaneous slopes and values of $z_M(t)$ and $z_E(t)$ as a function of time (see Figs. 10 and 11). These values of $z_M(t)$ and $z_E(t)$ appear to scale roughly linearly with $1/t$ implying $z \neq 0$, as was found in ref. [9], but the oscillating behavior near $t = 0$ makes difficult to make an accurate extrapolation for $1/t \rightarrow 0$ and compute an effective z . If the decay process were a pure power-law then according to the figures the values of z_M and z_E will be in the range $0.2 - 0.3$. In addition to the instantaneous slopes we also computed g_M (g_E) which are shown in Figs. 12 and 13. A linear fit of these data using Eq. 10, from $t = 1$ to $t = 80$, produced the following values,

$$b_M = 0.0043 \pm 0.0005 \quad (15)$$

$$\lambda_M = 0.28 \pm 0.01 \quad (16)$$

$$\Delta_M = 5.2 \pm 0.1, \quad (17)$$

and

$$b_E = 0.031 \pm 0.001 \quad (18)$$

$$\lambda_E = 2.2 \pm 0.1 \quad (19)$$

$$\Delta_E = 7.5 \pm 0.1. \quad (20)$$

These numbers agree well with the values of Hackl *et al*[19] for all the parameters except for Δ_E . The exponent b_M (b_E) was computed by evaluating Eq. 11 using the values of λ_M (λ_E) and Δ_M (Δ_E) from the g_M (g_E) fit and averaging \tilde{b}_M (\tilde{b}_E) from $t = 10$ to $t = 60$. This is shown in Figs. 14 and 15.

In Figs. 16 and 17 we have plotted the original data and the fit described by the ansatz. The power law/exponential ansatz, parameterized either with the values obtained in this paper or with Hackl *et al* values, describes the data reasonably well for initial and intermediate times although it appears to slightly underestimate the values for long times. To study this effect we repeated the analysis but now fitted the data from $t = 10$ to $t = 80$ in this way giving more weight to long time behavior. The fit produced somewhat different values for the magnetization parameters,

$$b_M = 0.0020 \pm 0.0005 \quad (21)$$

$$\lambda_M = 0.38 \pm 0.01 \quad (22)$$

$$\Delta_M = 7.0 \pm 0.1 \quad (23)$$

but basically identical ones for the energy,

$$b_E = 0.031 \pm 0.001 \quad (24)$$

$$\lambda_E = 2.2 \pm 0.1 \quad (25)$$

$$\Delta_E = 7.5 \pm 0.1 \quad (26)$$

In this case the ansatz for the magnetization fits better the data for long times as can be seen in Fig. 16. In fact, the $\lambda_M = 0.38$ implies $z_M = 0.33$ which is now closer to the value Tamayo found fitting a single power law decay. To expose this apparent different behavior of the short and long time magnetization data we performed an incremental fit of $g_M (g_E)$ vs $1/t$ always starting at $t = 1$ but ending at multiples of 10; the results are,

initial time	final time	Δ_M	λ_M	Δ_E	λ_E
1	11	4.70	0.253	7.58	2.22
1	21	4.94	0.267	7.52	2.20
1	31	5.04	0.273	7.52	2.20
1	41	5.11	0.278	7.52	2.20
1	51	5.18	0.280	7.52	2.20
1	61	5.20	0.283	7.52	2.20
1	71	5.22	0.284	7.52	2.20
1	81	5.29	0.288	7.52	2.20
1	91	5.33	0.291	7.52	2.20

Compare that with a similar incremental fit but now starting from $t = 10$,

initial time	final time	Δ_M	λ_M	Δ_E	λ_E
10	20	5.33	0.292	7.48	2.18
10	30	5.63	0.305	7.53	2.19
10	40	5.96	0.323	7.54	2.20
10	50	6.18	0.335	7.54	2.20
10	60	6.49	0.352	7.55	2.20
10	70	6.58	0.357	7.55	2.20
10	80	6.98	0.381	7.55	2.20
10	90	7.34	0.402	7.55	2.20

There are several conclusions we draw from this. The first is that the ansatz describes the energy relaxation very well. The energy results are consistent and very robust independent of the particular subset of data being used for the fit. For the magnetization the ansatz works well for short or intermediate times but for long times there is a trend by which the ansatz underestimates the data. This manifests as the change of values of Δ_M and λ_M as one adds longer time data points to the fit. Assuming this trend is significant then the behavior of the magnetization relaxation at long times might be more complex than expected. The variation of λ_M taken at face value indicates that the value of z_M falls in the interval $0.31 - 0.49$ for the time interval analysed and appears to vanish asymptotically. For the energy z_E appears to be around 0.45 and we didn't find evidence of a logarithmic factor.

In summary, we found evidence that exponential as well as power law factors are present in the relaxation of the energy and magnetization of large $2D$ Ising models with Swendsen-Wang dynamics. The ansatz proposed by Hackl *et al*, which combines an exponential factor with a power law, describes the energy relaxation very well. The magnetization relaxation is also described well for short and intermediate times but the behavior appears to be more complex at longer times.

The effect of different initial conditions (eg. $M(t = 0) \neq 1$), as has been studied in refs. [48, 49], was not considered here but will be the subject of future work.

Acknowledgments.

We want to thank L. Colonna-Romano, A. I. Melćuk, H. Gould, W. Klein, L. Tucker, R. Hackl and D. Stauffer, for comments and correspondence and J. Mesirov and B. Lordi of Thinking Machines Corp. for supporting this project. We wish to acknowledge the DOE Advanced Computing Lab. at Los Alamos, the Naval Research

Laboratory and Thinking Machines Corp. for providing the computer time that was needed to perform the simulations reported in this work.

References

- [1] C. Rebbi, Ed. *Lattice Gauge Theories and Monte Carlo Simulations*, World Scientific Singapore (1992).
- [2] K. Binder, Ed. *Monte Carlo Methods in Statistical Physics*, Springer-Verlag Berlin, New York (1986); K. Binder and D. W. Heermann. *Monte Carlo Simulation in Statistical Physics: an Introduction*, Springer-Verlag Berlin, New York (1988).
- [3] D. Stauffer and A. Aharony, *Introduction to Percolation Theory 2nd. ed.*, Taylor and Francis, London (1992).
- [4] D. Stauffer and H. E. Stanley, *From Newton to Mandelbrot: a Primer in Theoretical Physics*, Springer-Verlag Berlin, New York (1990).
- [5] D. C. Rapaport, *J. Phys. A* **18**, (1985) L175.
- [6] A. M. Ferrenberg and D. P. Landau, Critical Behavior of the Three-Dimensional Ising Model: a High-Resolution Monte Carlo Study *Phys. Rev. B* **44**, 5081 (1991).
- [7] C. F. Baillie, R. Gupta, K. Hawick and G. S. Pawley, Monte Carlo Renormalization-Group Study of the Three-Dimensional Ising Model *Phys. Rev. B* **45**, 10438 (1992); P. D. Coddington and C. F. Baillie, *Phys. Rev. Lett.* **68** (1992) 962.
- [8] A. N. Burkitt and D. W. Heermann, *Comp. Phys. Comm.* **54**, (1989) 210; D. W. Heermann and A. N. Burkitt, *Parallel Algorithms in Computational Science*, Springer Verlag, Heidelberg 1991.
- [9] P. Tamayo, *Physica A* **201**, 543 (1993).
- [10] C. F. Baillie and P. D. Coddington, *Concurrency: Practice and Experience* **3**(2), 129 (1991); C. F. Baillie and P.D. Coddington, *Phys. Rev. B* **43**, 10617 (1991);
- [11] R. C. Brower, P. Tamayo and B. York, *Jour. of Stat. Phys.* **63**, (1991) 73.
- [12] J. Apostolakis, P. Coddington and E. Marinari, *Europhys. Lett.* **17**(3), 198 (1992).
- [13] H. Mino, *Comp. Phys. Comm.* **66**, 25 (1991).
- [14] D. Stauffer, *Physica A* **171**, 471 (1991).
- [15] J. Kertesz and D. Stauffer, *Int. Jour. of Mod. Phys. C* **3**, 1275 (1992).
- [16] M. Flanagan and P. Tamayo, *Int. Jour. of Mod. Phys. C* **3**, 1235 (1992).
- [17] R. Hackl, H.-G. Matuttis, J. M. Singer, Th. Husslein and I. Morgenstern, *Parallelization of the 2D Swendsen-Wang Algorithm*, in: Large Scale Computational Physics on Massively Parallel Computers, H. J. Herrmann and F. Karsch Eds. World Scientific Pub. Co. LTD. p59 (1993); and *Int. Jour. of Mod. Phys. C*, December 1993.
- [18] M. Bauernfeind, R. Hackl, H.-G. Matuttis, J. M. Singer, Th. Husslein and I. Morgenstern, *3D Ising-Model with Swendsen-Wang Dynamics: A Parallel Approach*, preprint. To appear in *Physica A* 1994.
- [19] R. Hackl, H.-G. Matuttis, J. M. Singer, Th. Husslein and I. Morgenstern, *Efficient Parallelization of the 2D Swendsen-Wang Algorithm*, to appear in *Int. Jour. of Mod. Phys. C* 1994.
- [20] G. T. Barkema and T. MacFarland, *Phys. Rev. E* **50**, 1623 (1994).
- [21] R. Swendsen and J. S. Wang, *Phys. Rev. Lett.*, **58**, 86 (1987).
- [22] R. Brower and P. Tamayo, *Phys. Rev. Lett.*, **62**, 1087 (1989); R. Brower and S. Huang, *Phys. Rev. D* **41**, 708 (1990); U. Wolff, *Phys. Rev. Lett.* **60**, 1461 (1988); R. Edwards and A. Sokal, *Phys. Rev. D* **38**, 2009 (1988); W. Klein, T. Ray and P. Tamayo, *Phys. Rev. Lett.*, **62**, 163 (1989); P. Tamayo, R. C. Brower and W. Klein, *J. of Stat. Phys.*, **58**, 1083 (1990).
- [23] T. H. Cormen, C. E. Leiserson and R. L. Rivest, *Introduction to Algorithms*, MIT Press, (1990); D. Knuth, *The Art of Computer Programming*, vol 3, Addison-Wesley (1973).
- [24] E. Horowitz and S. Sahni, *Fundamentals of Computers Algorithms*, Potomac, Md. Computer Science Press, 1978.
- [25] Y. Shiloach and U. Vishkin, *Jour. of Algorithms* **3**, 57 (1982).

- [26] U. Vishkin, *Discrete Applied Mathematics* **9**, 197 (1984).
- [27] M. J. Quinn and N. Deo, *Computing Surveys*, Vol. 16, No 3, September 1984.
- [28] P. S. Gopalakrishnan, I. V. Ramakrishnan and L. N. Kanal, 1985 *IEEE, Int. Conf. on Parallel Processing*.
- [29] W. Lim, A. Agrawal and L. Nekludova, *Thinking Machines Tech. Report NA86-2*.
- [30] L. W. Tucker, Proc. *IEEE Conference on Computer Vision and Pattern Recognition*, June 1986, Miami, Florida.
- [31] J. Woo and S. Sahni, *Jour. of Supercomputing* **3**, (1989) 209.
- [32] H. Embrechts, D. Roose and P. Wambacq, *Hypercube and Distributed Computers*, F. Andre and J. P. Verjus eds. Elsevier Science Pubs. B. V. (North-Holland) 1989.
- [33] R. Cypher, J. L. C. Sanz and L. Snyder, *Journal of Algorithms* **10**, 140 (1989).
- [34] G. H. Blelloch, *Vector Models for Data-Parallel Computing*, MIT Press, 1990.
- [35] D. A. Bader and J. JáJá, Parallel Algorithms for Image Histogramming and Connected Components with an Experimental Study, Draft, University of Maryland 1994.
- [36] J. Greiner, A Comparison of Data-Parallel Algorithms for Connected Components, Tech. Rep. CMU-CS-93-191.
- [37] A. Choudhary and R. Thakur, *Jour. of Parallel and Dist. Comp.* **20**, 78 (1994).
- [38] John Apostolakis, Paul Coddington, Enzo Marinari, New SIMD Algorithms for Cluster Labeling on Parallel Computers, NPAC technical report SCCS-279 (1992).
- [39] A. Coniglio and W. Klein, *J. Phys. A*, **13**, (1980) 2775. p
- [40] A. Coniglio, *Phys. Rev. Lett.*, **62**, (1989) 3054.
- [41] J. Hoshen and R. Kopelman, *Phys. Rev. B*, **14**, (1976) 3438.
- [42] U. Wolff, *Phys. Lett. B* **228**, (1989) 379 .
- [43] C. Munkel, *Int. Jour. of Mod. Phys. C* **4**, 79 (1993).
- [44] H. J. Herrmann and H. E. Stanley, *J. Phys. A* **21** L829 (1988).
- [45] E. N. Miranda, *Physica A* **175**, 235 (1991), **179**, 340 (1991); *Physica A* **175**, 229 (1991).
- [46] D. Stauffer and J. Kertesz, *Physica A* **177**, 381 (1991).
- [47] R. Hackl, Personal Communication.
- [48] L. Colonna-Romano, A. I. Melćuk, H. Gould, and W. Klein, *Physica A* **209**, 396 (1994).
- [49] H. K. Janssen, B. Schaub and B. Schmittmann, *Z. Phys. B* **73**, 539 (1988).

This figure "fig1-1.png" is available in "png" format from:

<http://arxiv.org/ps/hep-lat/9502007v1>

This figure "fig2-1.png" is available in "png" format from:

<http://arxiv.org/ps/hep-lat/9502007v1>

This figure "fig2-2.png" is available in "png" format from:

<http://arxiv.org/ps/hep-lat/9502007v1>

This figure "fig1-4.png" is available in "png" format from:

<http://arxiv.org/ps/hep-lat/9502007v1>

This figure "fig1-5.png" is available in "png" format from:

<http://arxiv.org/ps/hep-lat/9502007v1>

This figure "fig1-6.png" is available in "png" format from:

<http://arxiv.org/ps/hep-lat/9502007v1>

This figure "fig1-7.png" is available in "png" format from:

<http://arxiv.org/ps/hep-lat/9502007v1>

This figure "fig1-8.png" is available in "png" format from:

<http://arxiv.org/ps/hep-lat/9502007v1>

This figure "fig1-9.png" is available in "png" format from:

<http://arxiv.org/ps/hep-lat/9502007v1>

This figure "fig1-10.png" is available in "png" format from:

<http://arxiv.org/ps/hep-lat/9502007v1>

This figure "fig1-11.png" is available in "png" format from:

<http://arxiv.org/ps/hep-lat/9502007v1>

This figure "fig1-12.png" is available in "png" format from:

<http://arxiv.org/ps/hep-lat/9502007v1>

This figure "fig1-13.png" is available in "png" format from:

<http://arxiv.org/ps/hep-lat/9502007v1>

This figure "fig1-14.png" is available in "png" format from:

<http://arxiv.org/ps/hep-lat/9502007v1>

This figure "fig1-15.png" is available in "png" format from:

<http://arxiv.org/ps/hep-lat/9502007v1>

This figure "fig1-16.png" is available in "png" format from:

<http://arxiv.org/ps/hep-lat/9502007v1>

This figure "fig1-17.png" is available in "png" format from:

<http://arxiv.org/ps/hep-lat/9502007v1>

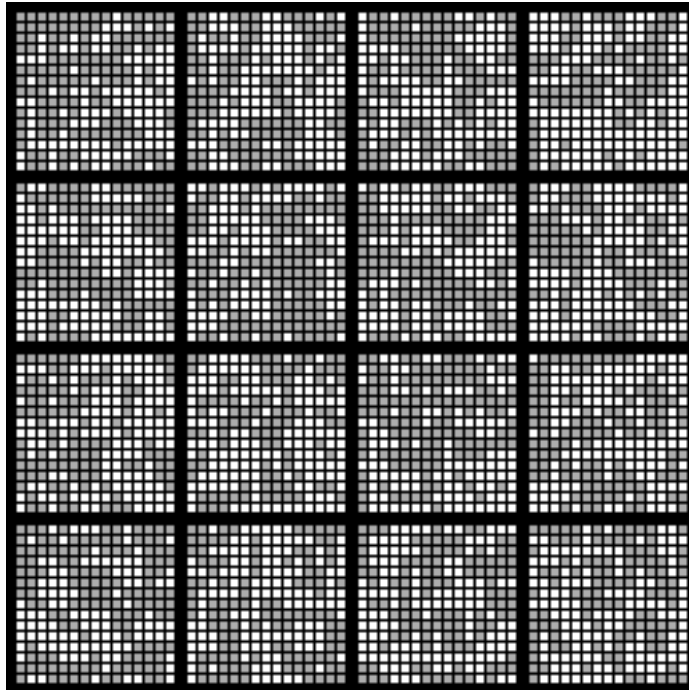


Fig 1.- Partitioning of a 64 x 64 lattice of spins into 16 cell domains. Each cell domain is assigned to a processor.

Fig. 2.- Initial and final stages of the Local-Labeling procedure for one processor. The initial condition on top shows the sites connected by percolation (connectivity) bonds. The second figure shows the result of the local labeling where each site points to its local root. At the bottom the local roots are globalized (i.e. made unique over the whole system) and boundary pointers are set up for the relaxation process.

Fig. 3.- The global relaxation process set up is shown for a subsystem of four processors. Each processor exchanges root labels with nearest neighbors. Labels are compared and set to minimum values. The process is repeated until no more changes in the labels are detected.

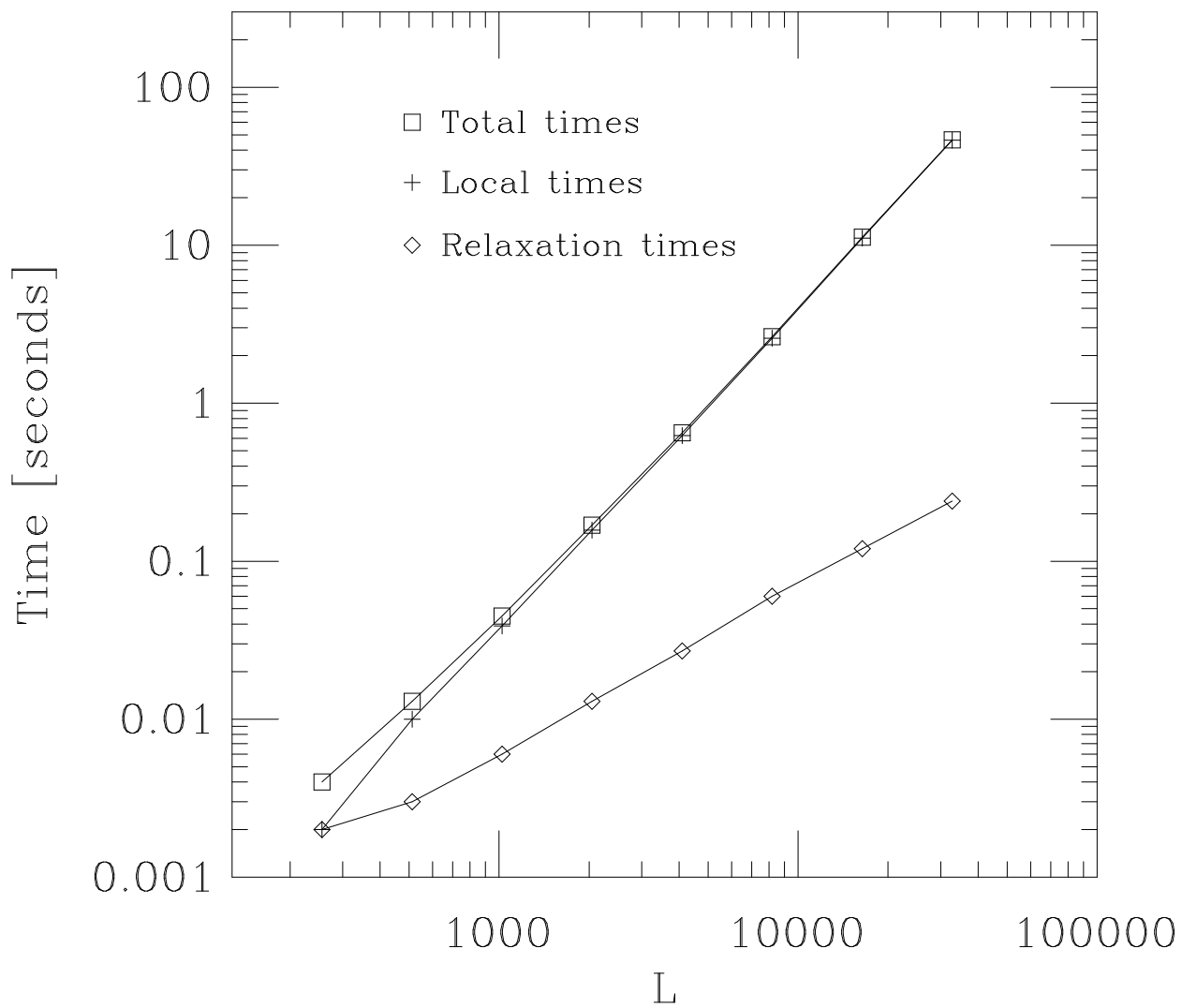


Fig. 4.- Local, relaxation and total times as a function of lattice size on a 64-node CM-5E supercomputer.

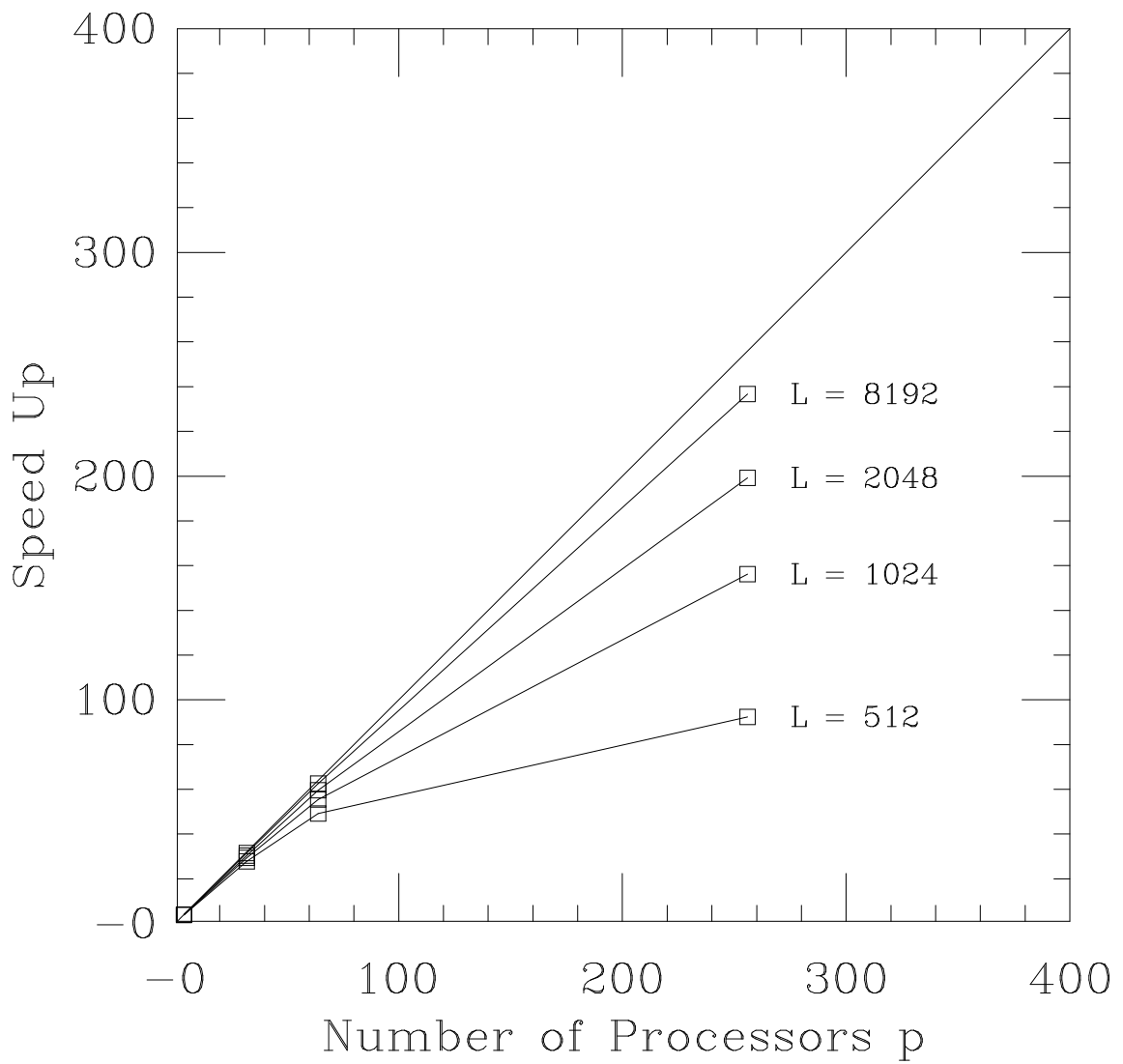


Fig. 5.- Speed-up function for different lattice sizes. The straight line ($S_p = p$) shows the ideal linear speed-up.

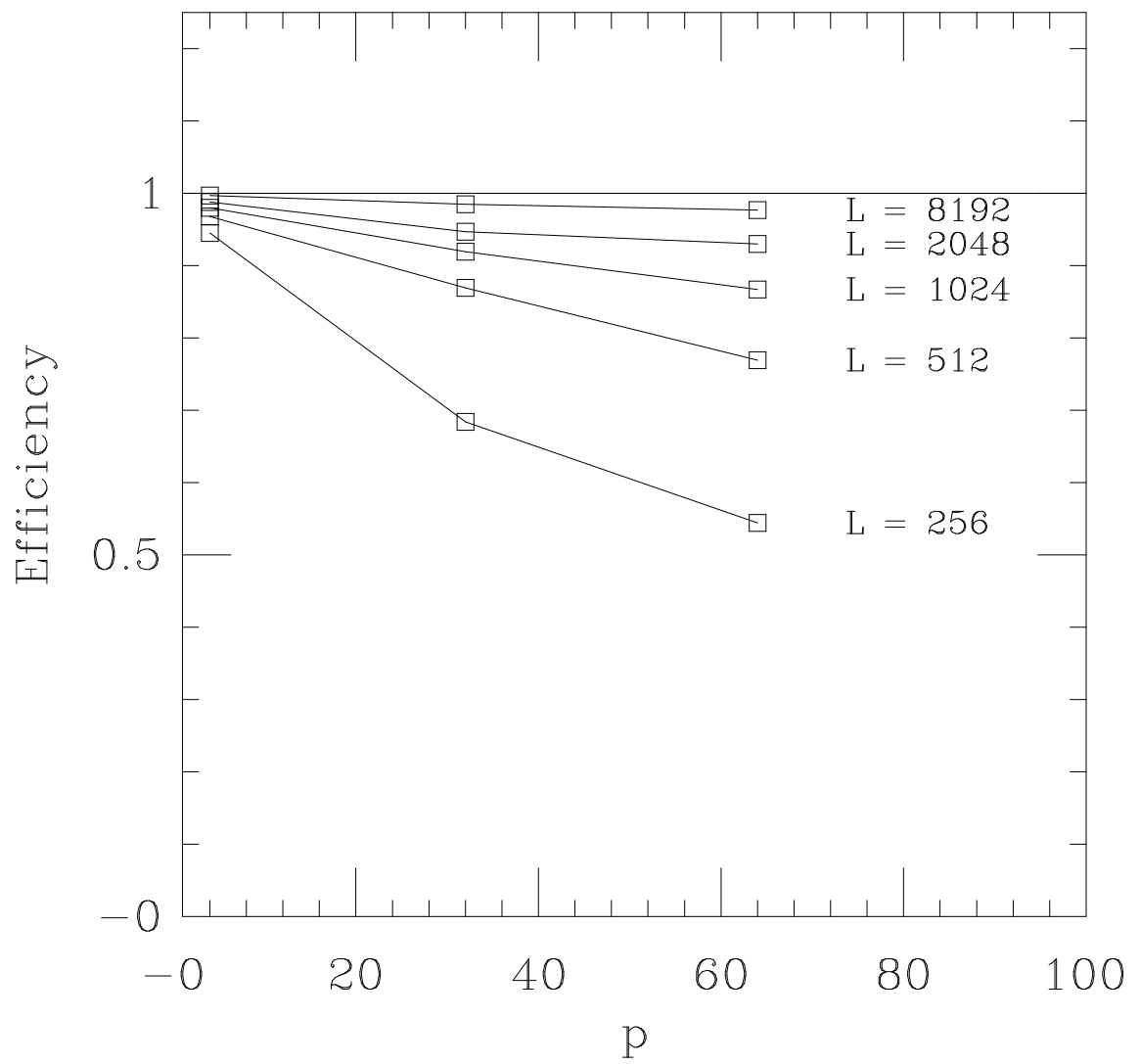


Fig. 6.- Efficiency (S_p/p) function for different lattice sizes.

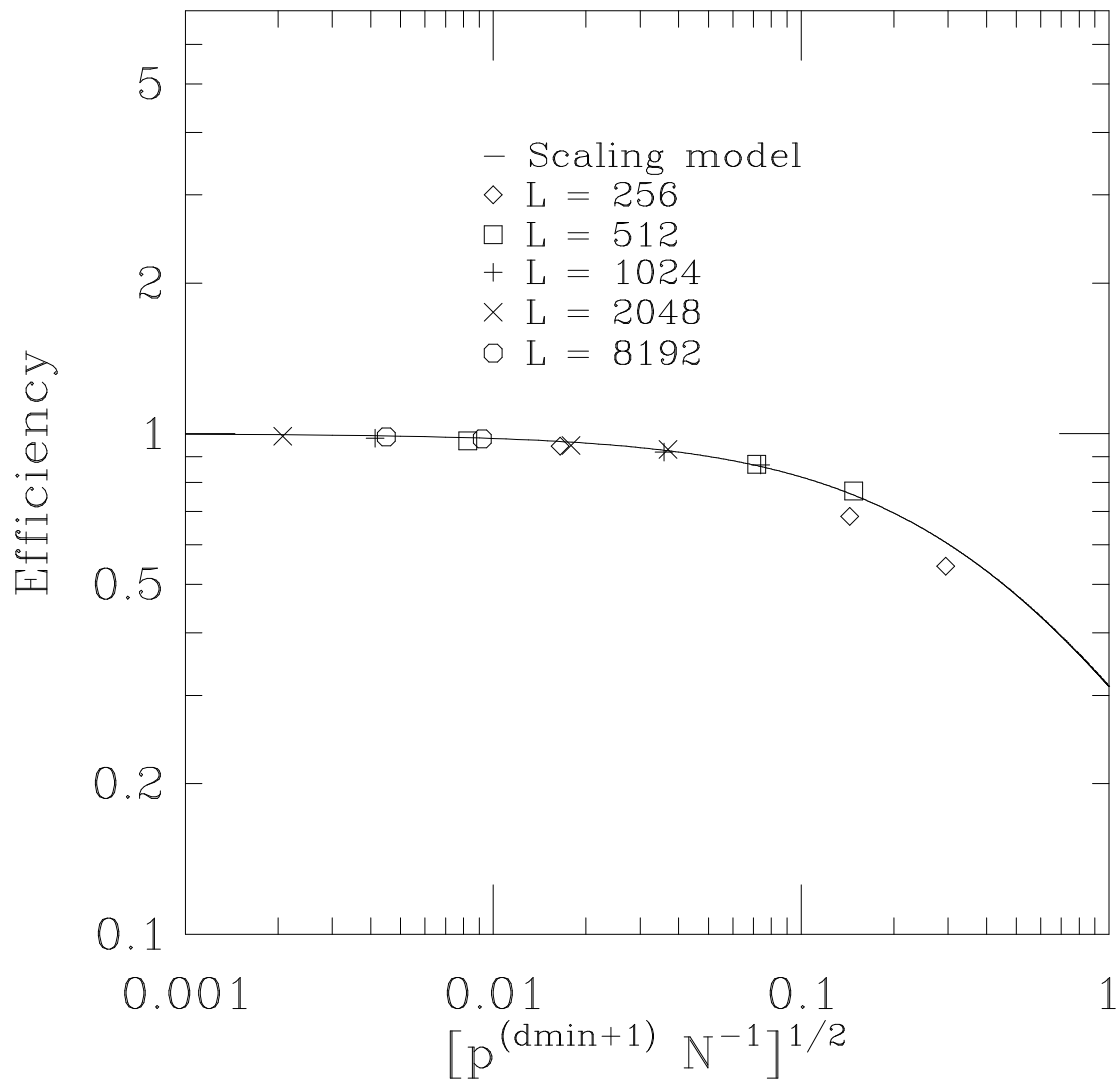


Fig. 7.- Universal form of the efficiency function.

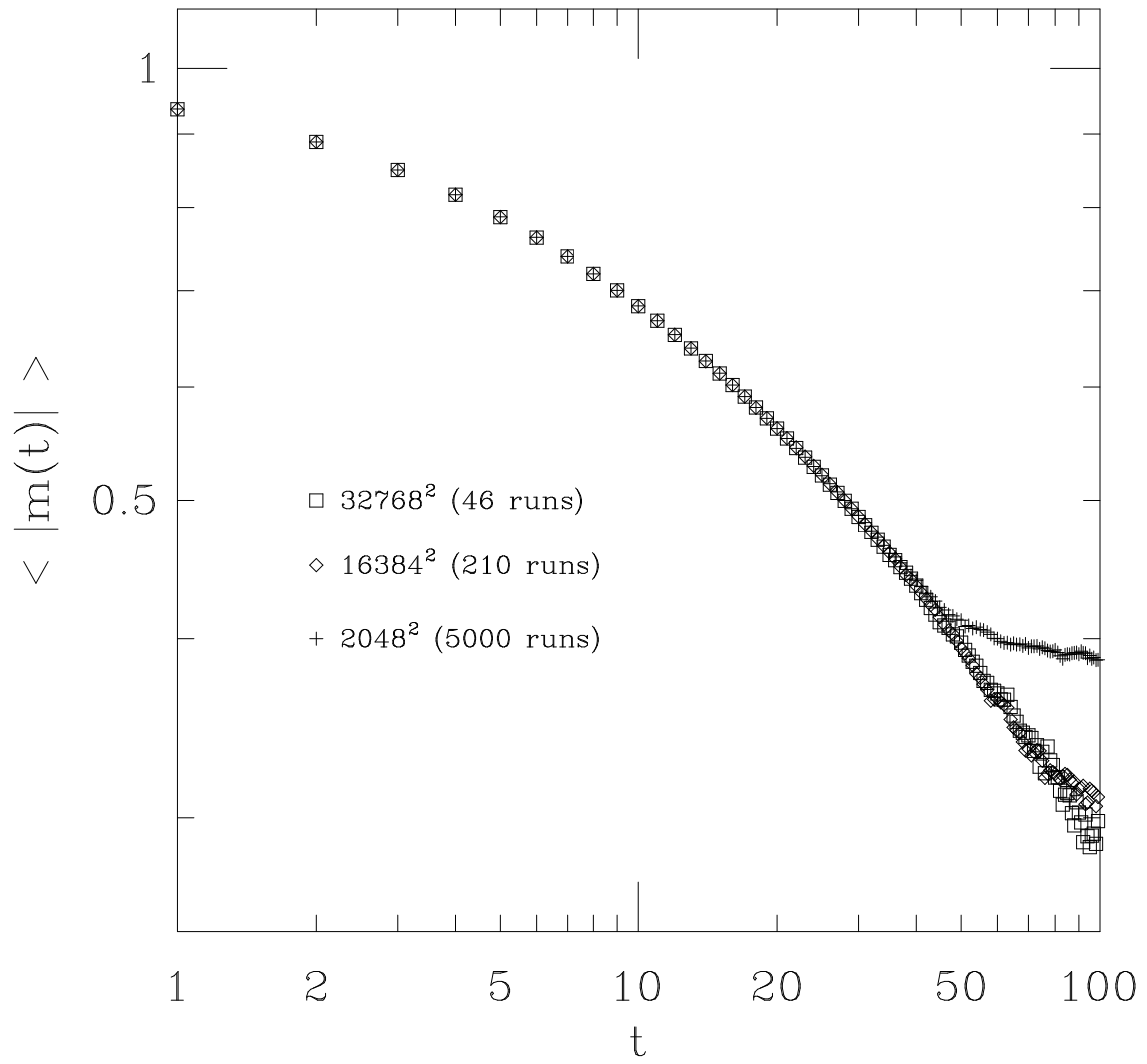


Fig. 8.- Magnetization relaxation data for different lattice sizes.

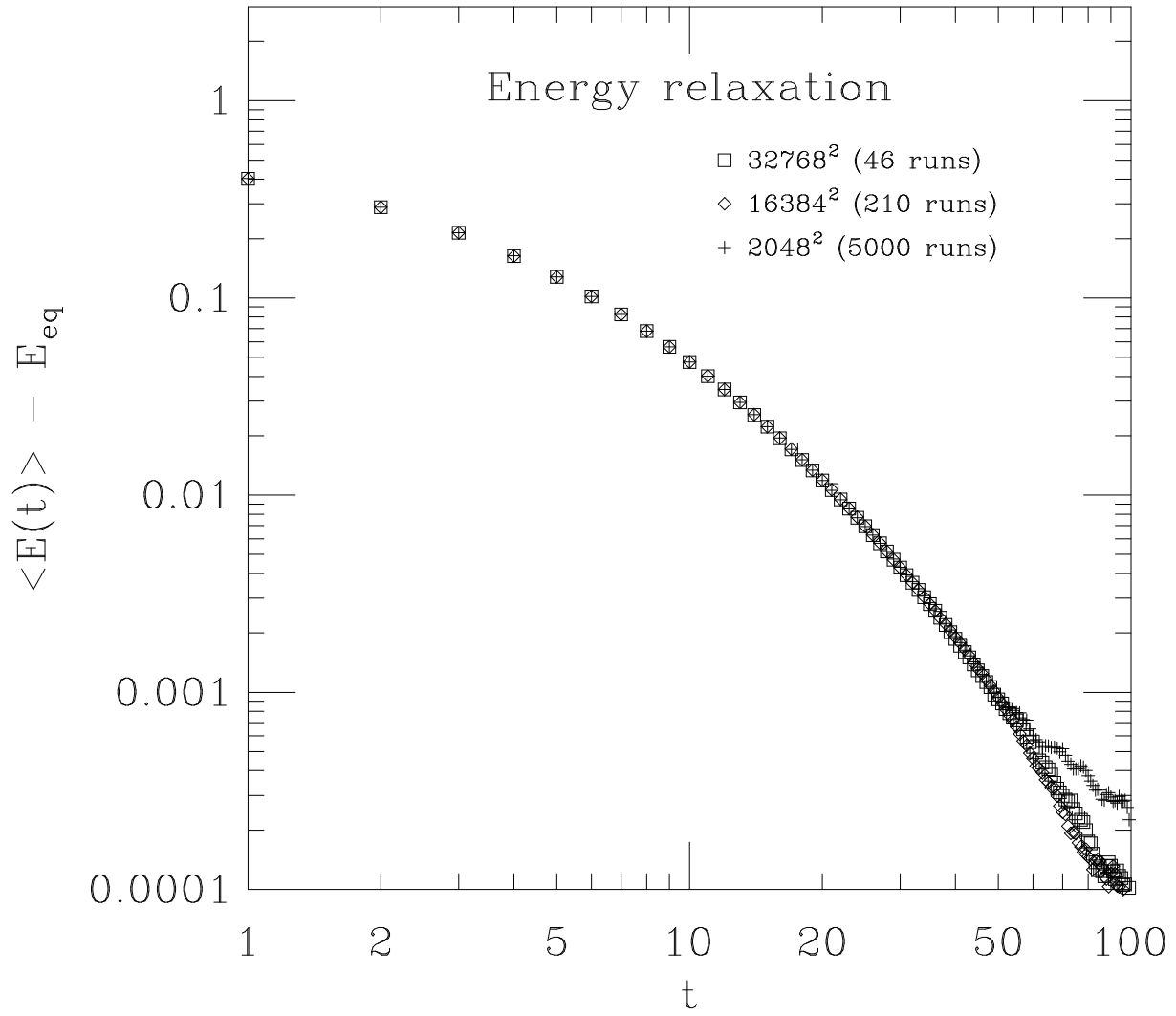


Fig. 9.- Energy relaxation data for different lattice sizes.

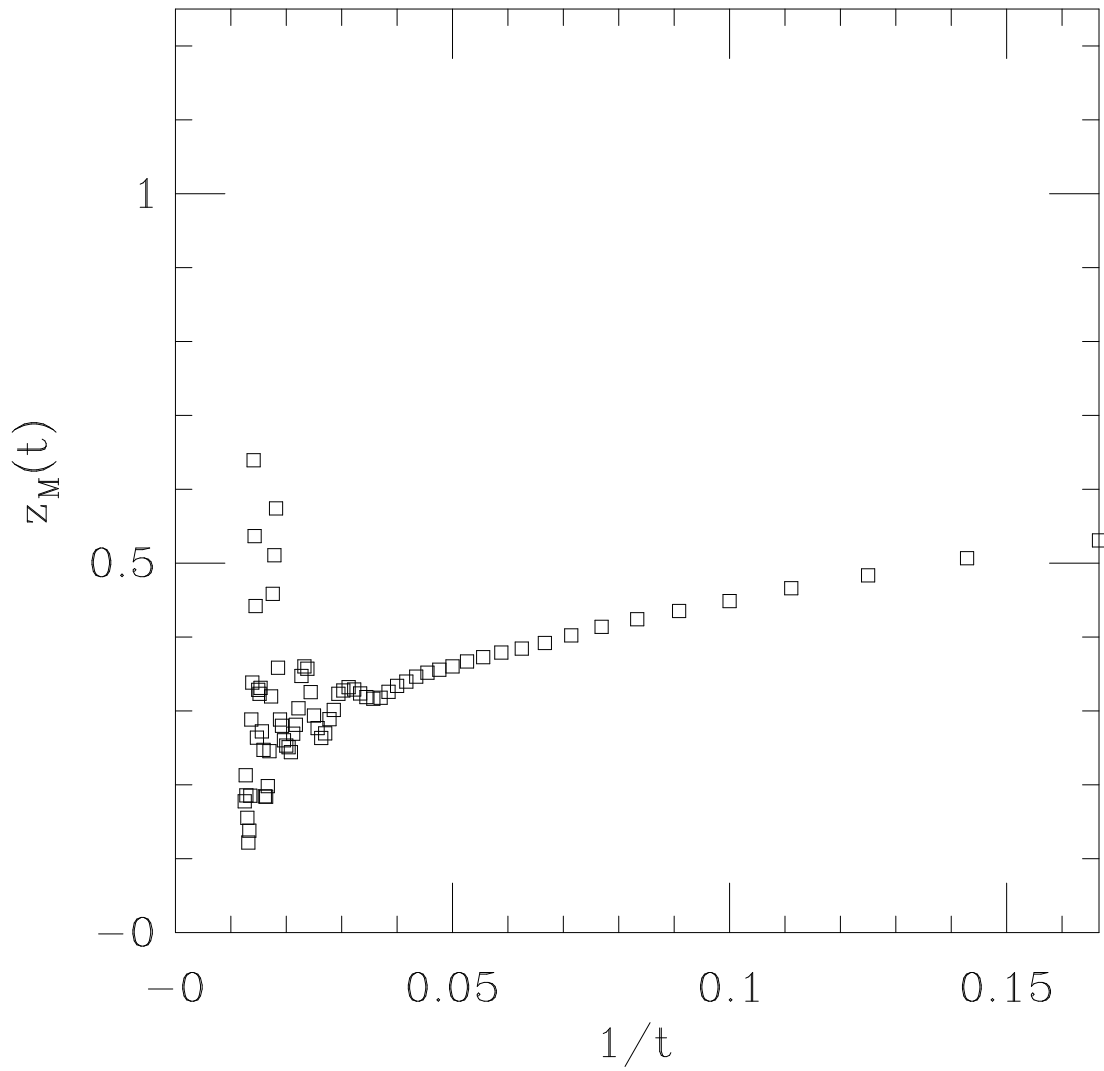


Fig. 10.- Time dependent $z_M(t)$ exponent computed from the instantaneous slope as a function of $1/t$.

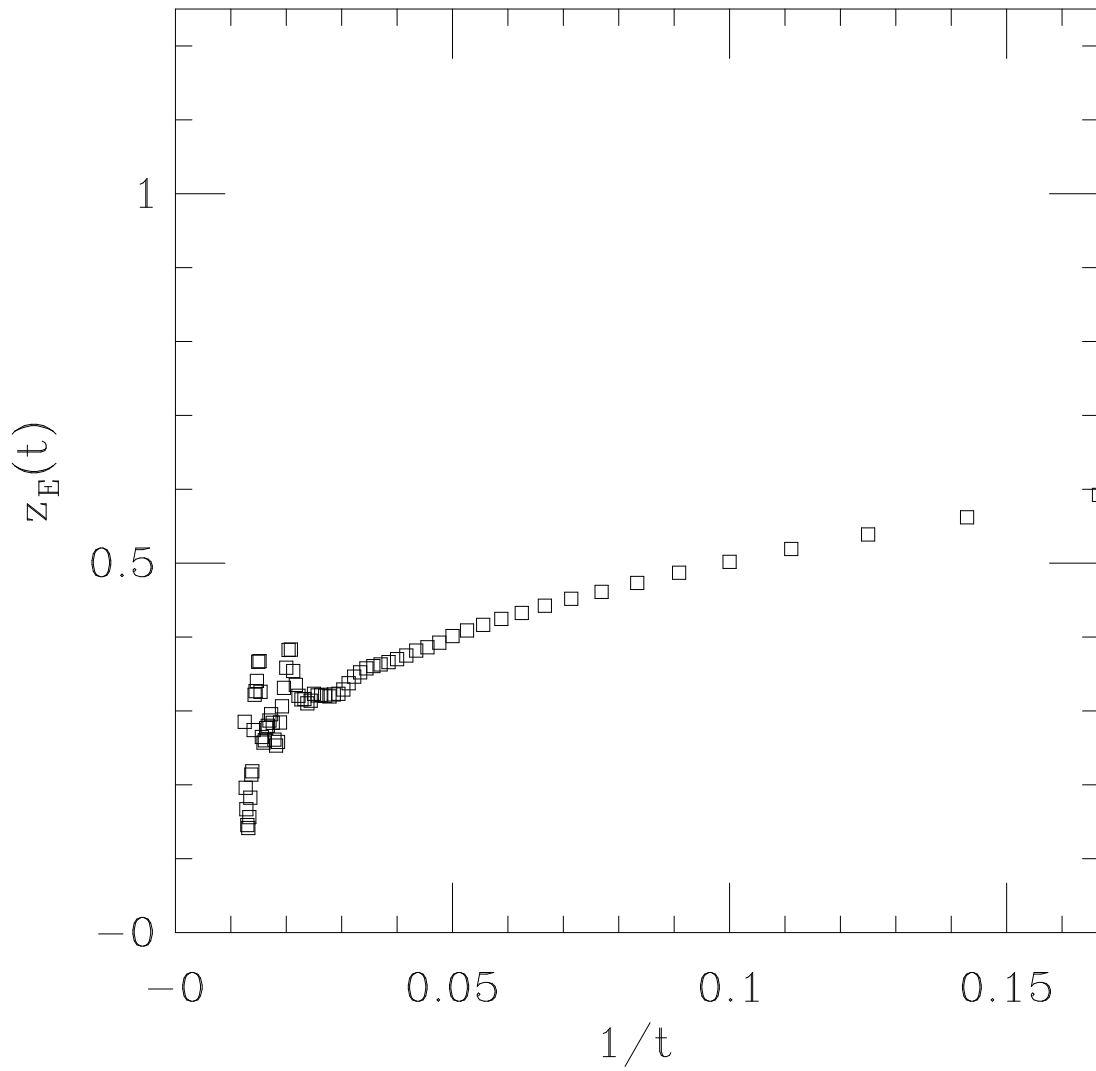


Fig. 11.- Time dependent $z_E(t)$ exponent computed from the instantaneous slope as a function of $1/t$.

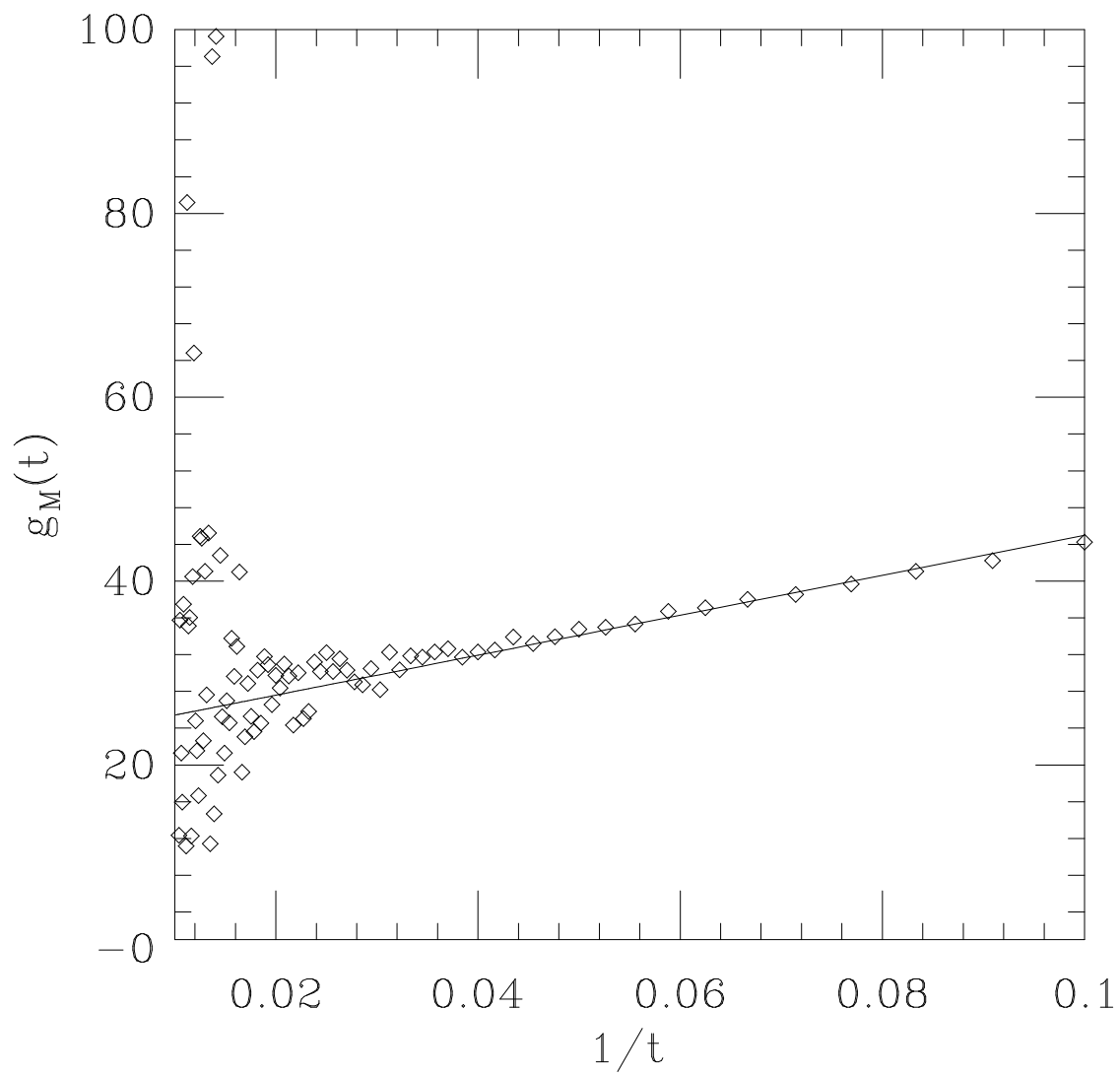


Fig. 12.- Auxiliary function $g_M(t)$. The solid line shows the linear least-squares fit.

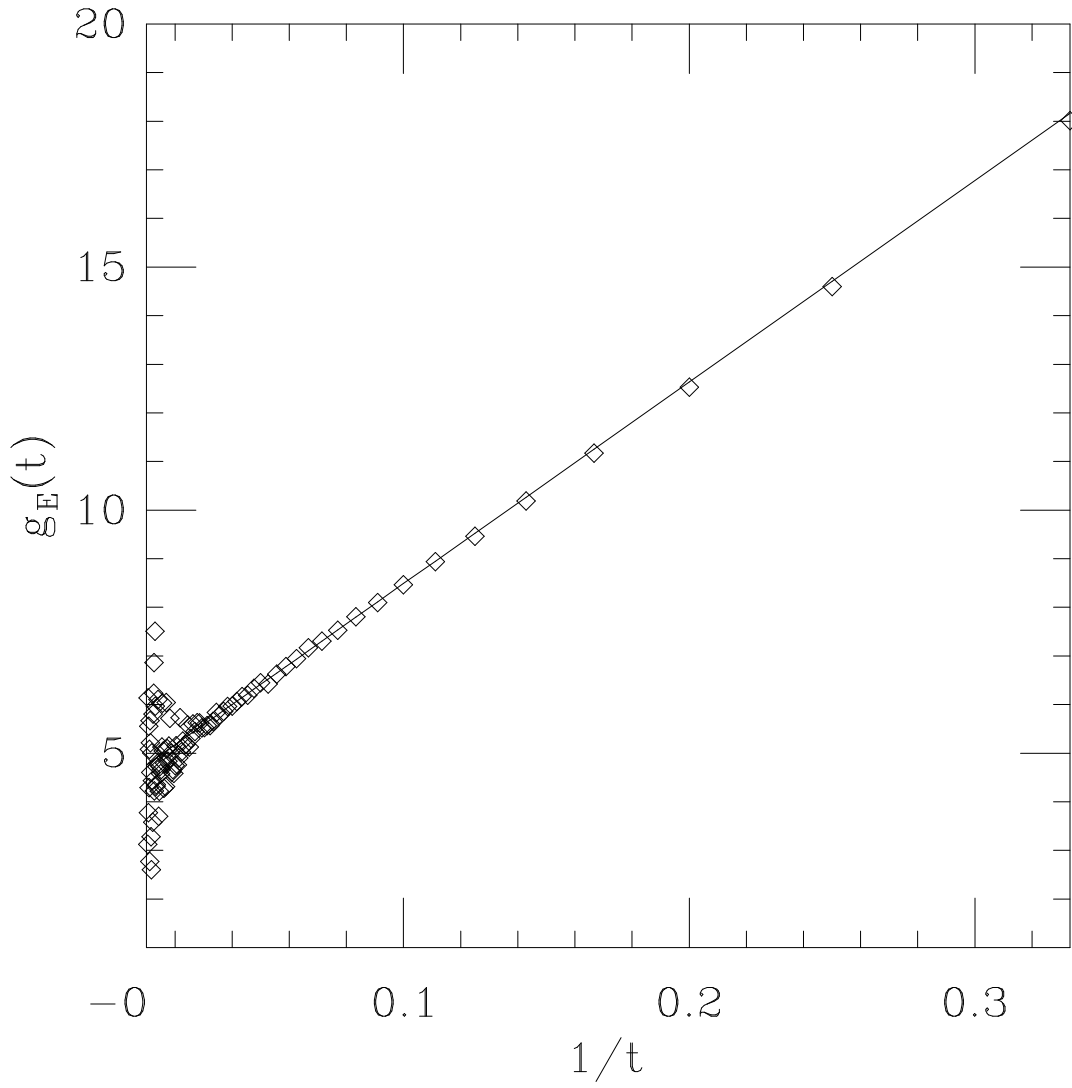


Fig. 13.- Auxiliary function $g_E(t)$. The solid line shows the linear least-squares fit.

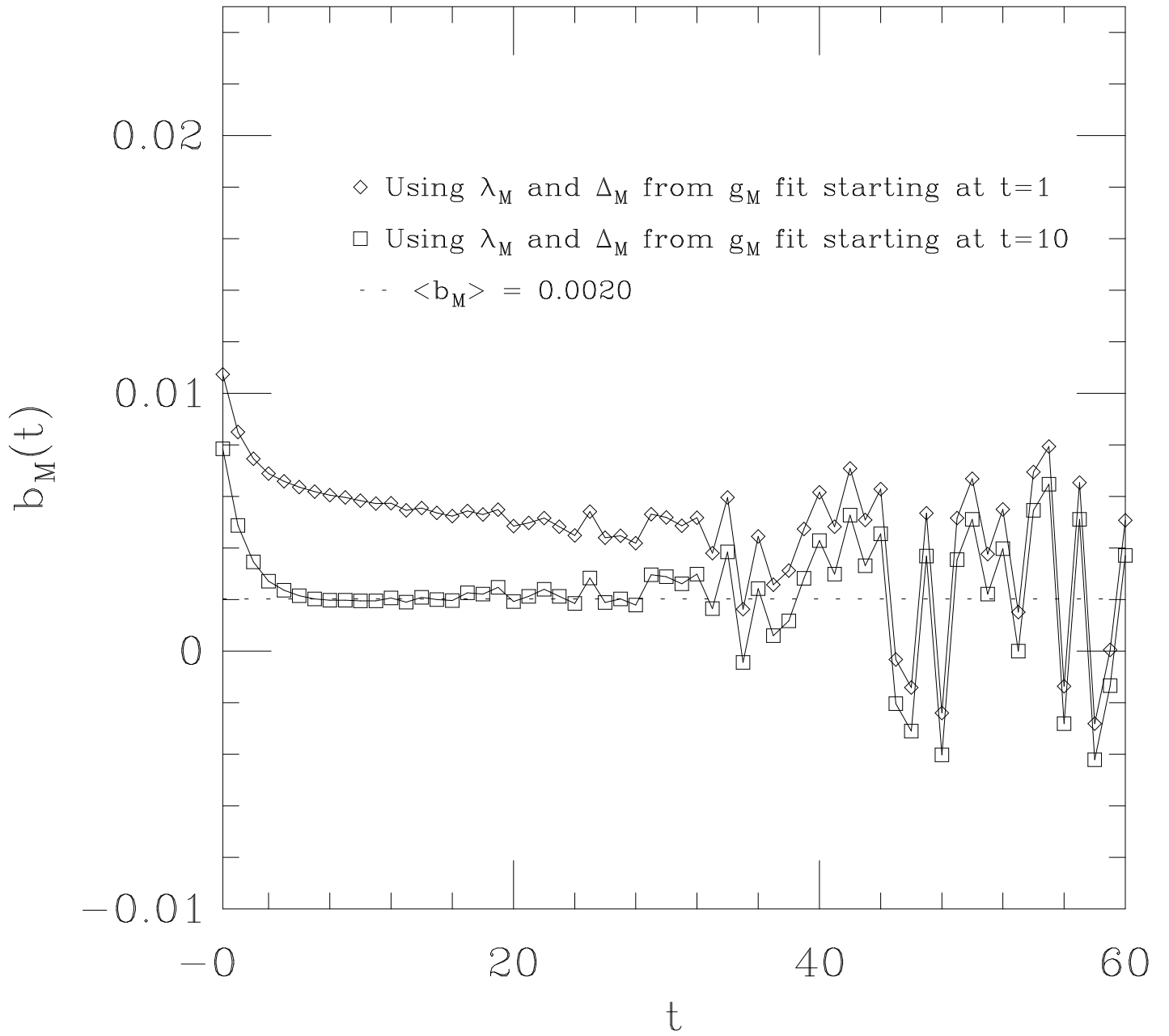


Fig. 14.- Exponent $b_M(t)$ as a function of time.

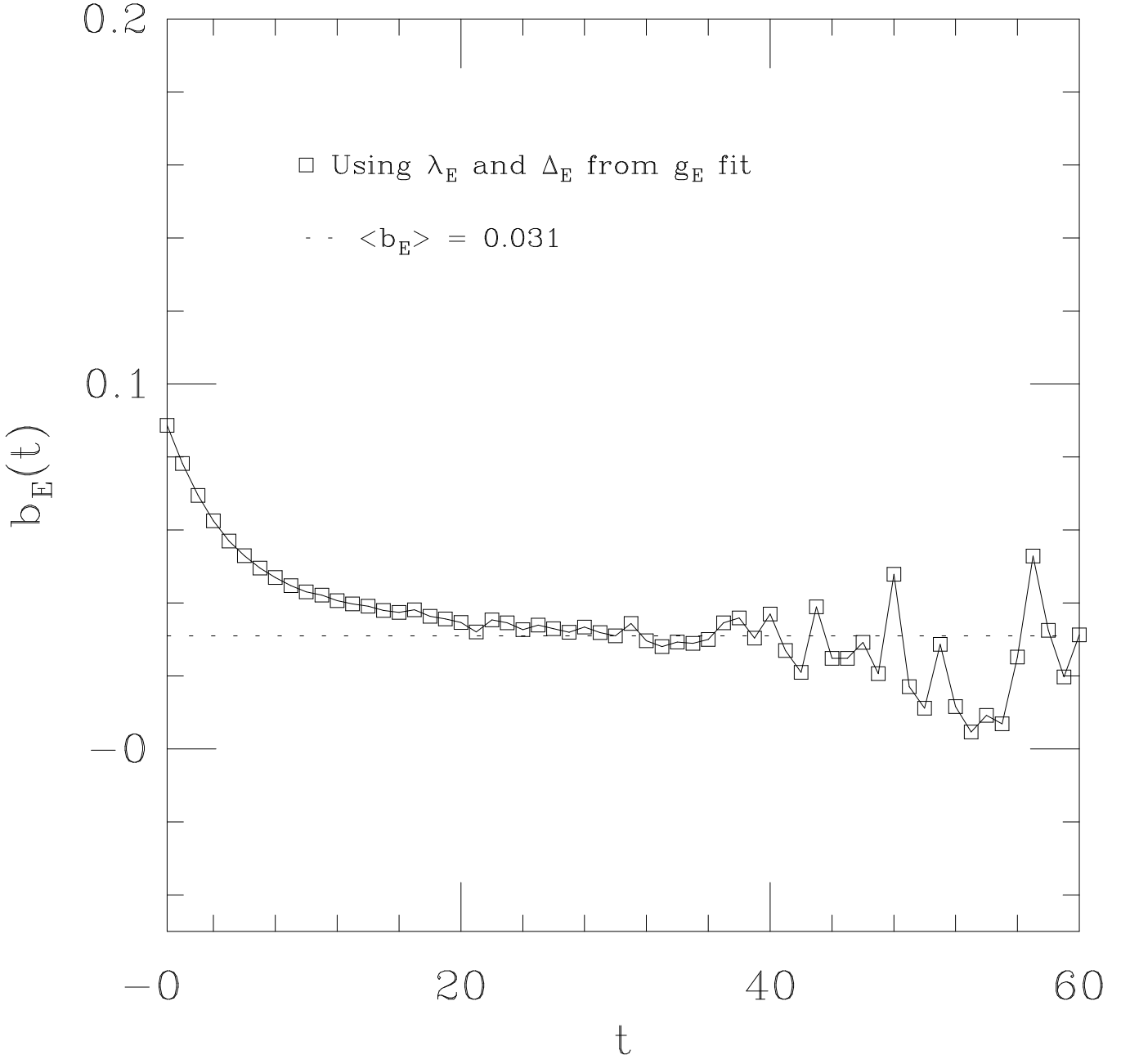


Fig. 15.- Exponent $b_E(t)$ as a function of time.

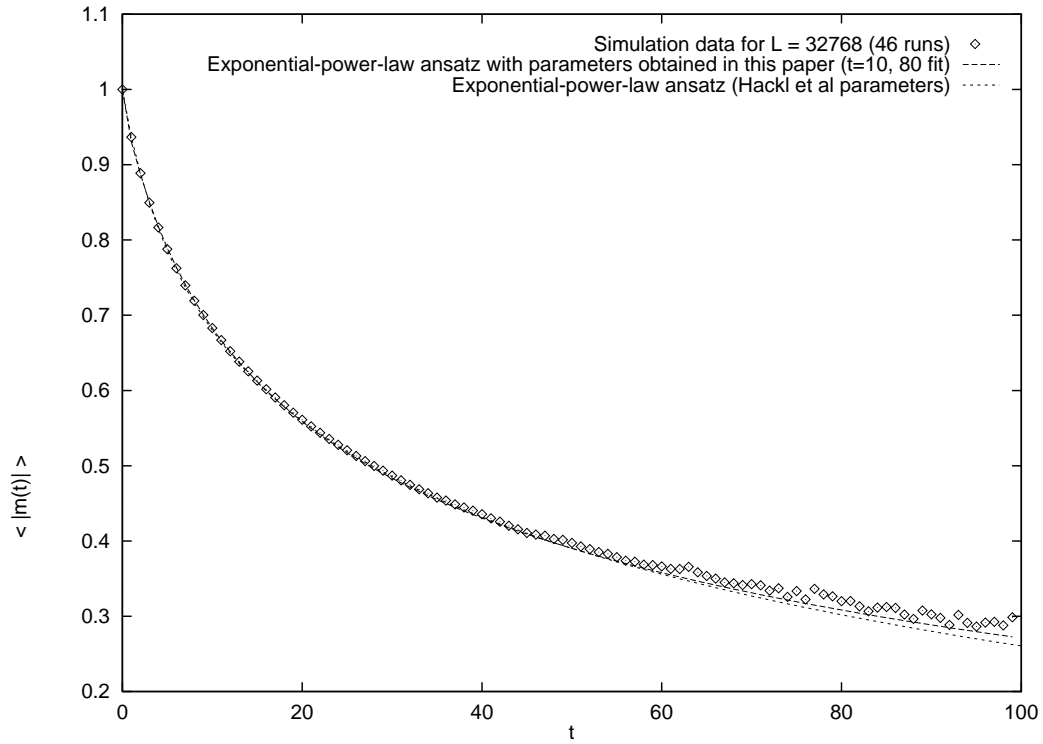


Fig. 16.- Magnetization relaxation data for $L=32768$. The model (ansatz) parameterized with the values obtained in this paper and Hackl *et al* values are also shown.

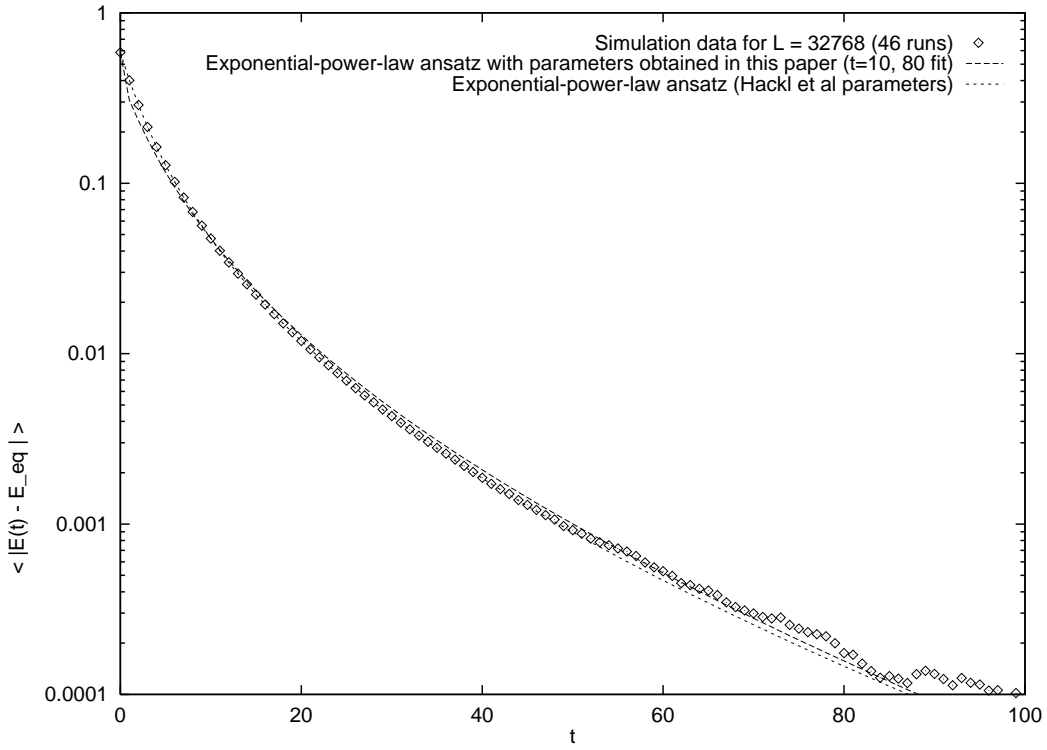


Fig. 17.- Energy relaxation data for $L=32768$. The model (ansatz) parameterized with the values obtained in this paper and Hackl *et al* values are also shown.